VERTICAL FLOW OF GAS AND LIQUID MIXTURES IN WELLS

H. Duns Jr. * – N. C. J. Ros **

Abstract. The need and importance of accurate prediction and analysis of pressure variations along the length of the flow string in oil wells, and the various ways in which this problem has been dealt with in the past are discussed in an introductory note. Thereafter a new, more general, approach based on extensive laboratory experiments is presented.

It is expected that the resulting new correlation and its associated calculating procedure represent a considerable improvement over existing methods and can be applied over the full range of field operating conditions: tubing and annular flow for a wide range of oil and gas mixtures with varying water cuts.

The correlation which has been developed for one of the flow regimes of oil and gas, i. e. "mist flow", is applicable to gas/condensate wells and can presumably be used also in gas/condensate wells with a water cut, provided that no emulsion is formed.

It is realized that the new correlations are of a complicated nature but, fortunately, the intricacies of the formulae are of little importance when an electronic computer is used.

Résumé. Le besoin et l'importance de pronostics et d'analyses exactes des variations de pression tout le long de la colonne d'extraction dans les puits de pétrole, et les manières différentes de résoudre ce problème sont traitées dans une note introductoire. Ensuite on a exposé une nouvelle manière d'aborder le problème, plus générale, et basée sur des expériences de laboratoire effectuées à une grande échelle.

Il est escompté que la nouvelle corrélation qui en résulte et la façon de calculer qui en dépend représentent une amélioration considérable par rapport aux méthodes existantes et pourront être mises en oeuvre pour la gamme entière des conditions de travail: tubage et écoulement annulaire pour une grande gamme de mélanges huile et gaz avec différentes teneurs d'eau.

La corrélation qui a été mise au point pour un des régimes d'écoulement d'huile et de gaz, dit «écoulement à l'état de brume», est applicable aux puits de gaz/condensats et peut vraisemblablement être utilisée également dans des puits de gaz/condensats ayant une certaine teneur d'eau, pourvu qu'aucune émulsion ne se soit formée.

Il est constaté que les nouvelles corrélations sont compliquées, mais heureusement la complexité des formules se résout facilement par l'utilisation d'une calculatrice électronique.

I. Introduction

A. Importance of energy losses in vertical flow

In the flow of oil from the reservoir rock to the surface tanks, three completely different stages of flow can be discerned:

1. radial liquid and/or gas-liquid flow through the permeable reservoir rock to the well bore;
2. vertical liquid and/or gas-liquid flow through a circular or annular conduit from the bottom of the well to the well head;
3. horizontal gas-liquid flow through the surface lines and facilities to the tanks.

In each of these stages the behaviour of the flow is different and the corresponding pressure losses are governed by a different set of factors. In this paper only the vertical flow stage will be dealt with.

Analysis of the utilization of available pressure by the flow from the reservoir to the surface tanks will show that the major portion is generally used in the vertical flow stage. This is shown in Table I for a well

* Duns, H. / Netherlands / Civil Engineer / Techn. Univ. at Delft / Head of Production Engineering, Advisory Unit B.I.P.M., The Hague.
** Ros, N. C. J. / Netherlands / Mechanical Engineer / Techn. Univ. at Delft / Research Engineer, Koninklijke Shell Exploratie en Produktie Laboratorium, Rijswijk.

of 10,000 ft with a static bottom hole pressure of 3,000 psi, a gas-oil ratio of 750 cf/b, producing through 3.1/2" O.D. tubing, against a well head pressure of 200 psi, for four different productivity indices (P.I.'s).

TABLE I

PRESSURE LOSS DISTRIBUTION IN OIL FLOW

Productivity Index (b/d per psi)	Production (b/d)	Percentage Loss of Total Available Pressure in		
		Reservoir	Tubing	Surface lines
2.5	2700	36	57	7
5	3700	25	68	7
10	4500	15	78	7
15	4800	11	82	7

It is evident from this example that, for deep wells with large P.I.'s in particular, the portion of the pressure absorbed by the vertical flow performance becomes of major importance.

In the search for oil there is a trend born out of necessity to explore at ever increasing depths and in quite often highly inaccessible areas such as deserts and off-shore regions. The large capital requirements associated with this exploration can only render a reasonable return on the investment when the wells are produced at maximum rates consistent with good engineering practice, thus where a great part of the available pressure is utilized in the vertical flow stage.

When production by natural flow ceases it may be sustained by means of gas lift, which normally is the second best method to produce high rates of flow from deep horizons. In this method of production, the greater part of the pressure losses also occur in the vertical flow stage.

Therefore, the ability to analyse and predict flowing and gas-lift well performances is to a great extent dependent on the availability of reliable gas-liquid vertical flow pressure traverses.

B. Gas-liquid vertical flow

In contrast to liquid flow, pressure losses in gas-liquid vertical flow do not always increase with an increase in production rate or with a reduction of the conduit size. This is due to the presence of gas which tends to slip through the liquid column without contributing to its lift. This phenomenon can best be visualized by a large tank filled with oil and through the centre of which gas is bubbling. The gas will not lift the oil out of the tank but just slip through it. On reduction of the diameter of the tank, however, a point will be reached where the oil will be lifted out of the tank by the gas bubbles.

From both field measurements and laboratory experiments it has been found that in gas-liquid vertical flow, minimum pressure losses over the vertical string can be obtained:

a) for a given rate of flow and conduit size at one specific Gas-Liquid Ratio (GLR);
b) for a given GLR and conduit size at one specific rate of flow;
c) for a given GLR and rate of flow at one specific conduit size.

C. Use of gas-liquid vertical pressure traverses

In the evaluation of flowing and gas-lift wells the graphical method of analysis, using vertical pressure traverses, as originally suggested by Gilbert has proved to be of great value and is amply described[1]). Specific application to gas-lift problems has been reported by McAfee[2]).

Once reliable pressure traverses have become available for a wide range of field operating conditions, these can be successfully applied for appropriate conduit-size selection, prediction of flowing and gas-lift life of a well, prediction of economically recoverable oil by flowing and/or gas-lift, calculation of flowing bottom hole pressures (and thus productivity indices) from flowing well head pressures and checking of gauging data.

In Fig. 1 pressure traverses are shown for a gas-oil ratio of 600 cf/b for three different conduit sizes. For a well, 5000 ft deep and producing at this GOR, the intake pressure at the tubing intake for a rate of 5000 b/d would have to be 2900, 1400 and 850 psi for 2.3/8" O.D., 3.1/2" O.D. tubing and 7" x 2.7/8" annulus conduit sizes respectively (points A, B, and C in Figure 1) when producing against a well head pressure of 200 psi, thus illustrating that high rate natural flow could be maintained much longer through the annular conduit than, for instance, through 2.3/8" O.D. tubing.

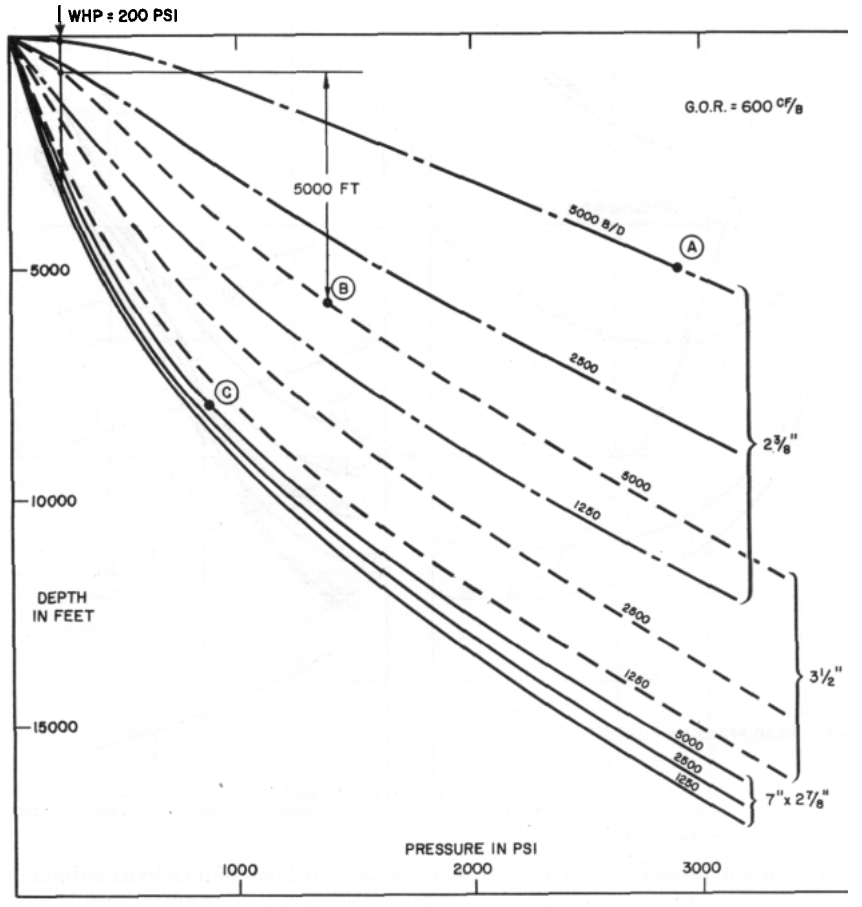

Figure 1 Flowing pressure traverses for three conduit sizes and one gas oil ratio.

An example of the determination of the life of a flowing well, and of a gas lift well, is given in Fig. 2. The well is equipped with 10,000 ft of 2.7/8" O.D. tubing.

The tubing intake pressures, which are required to lift a certain production rate at different GOR's against a well head pressure af 200 psi, have been plotted in Fig. 2A, using the available pressure traverses for 2.7/8" O.D. tubing. From this graph, Fig. 2B can be constructed where the required intake pressures at 10,000 ft are plotted against production rate using the GOR as parameter.

In both figures the Optimum GOR-line is drawn (dotted line) which indicates, in the case of Fig. 2A that GOR which will render a minimum intake pressure for a certain rate and in the case of Fig. 2B the lowest possible value of the intake pressure for different rates.

To facilitate the determination of the value of the Optimum GOR for a given rate of production, Fig. 2C is added at the bottom of Fig. 2B.

The advantage of Figures 2B and 2C is that all the required information can now be quickly read off by super-imposing the reservoir inflow performance, i. e. the pressures which can be supplied by the reservoir at the tubing intake depth at different rates of production, for the successive stages of depletion of the reservoir.

Suppose a reservoir engineering analysis of the above well has shown that the trend of the static bottom hole pressure (S.B.H.P.), the P.I. and the GOR for various cumulative withdrawals will be as follows: —

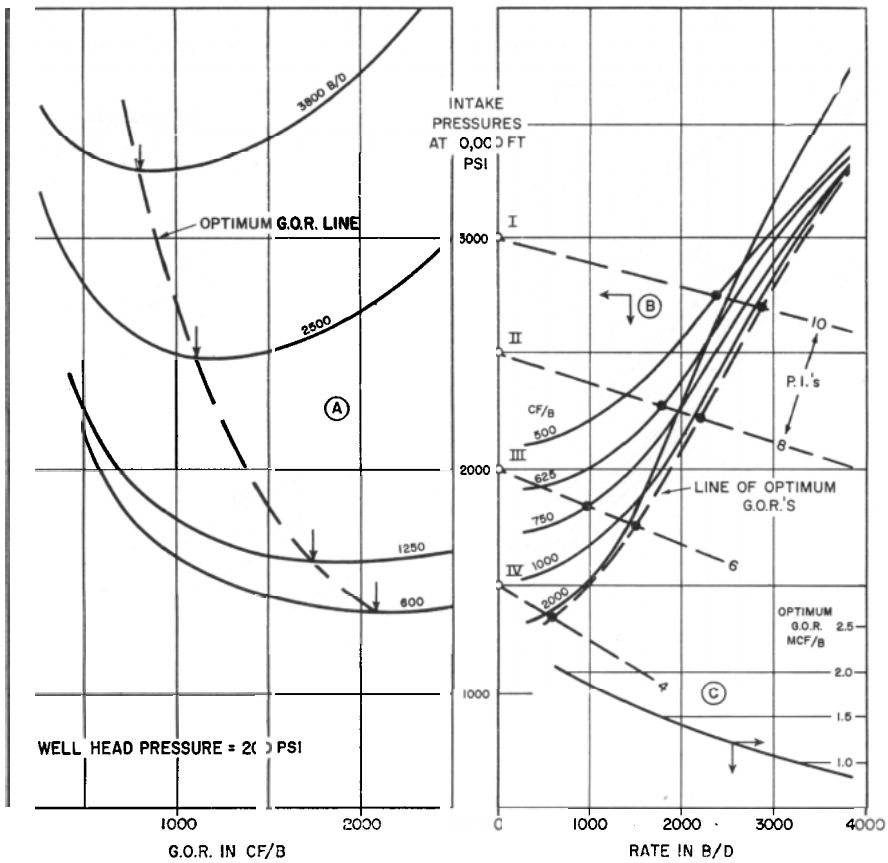

Figure 2. Intake pressure lines for 2.7/s" O.D. tubing with rate and GOR as parameter

TABLE II

RESERVOIR PRODUCTION DATA

Stage	Cumulative production (bbls)	SBHP at 10,000 ft (psi)	P.I. (b/d per psi)	G.O.R. (cf/b)
I	0	3.000	10	500
II	200.000	2.500	8	625
III	350.000	2.000	6	750
IV	450.000	1.500	4	1000

The inflow performance lines for the stages I–IV are indicated by their corresponding P.I.'s in Fig. 2B.

The production rates, which may be obtained on Natural Flow and/or Optimum Gas Lift, the respective lives of both methods of production, the required gas injection pressures at the tubing intake, and gas lift gas requirements can now be read off.

For instance at the beginning of the well's life the intersection of the inflow performance line for a P.I. of 10 b/d per psi with the intake pressure line for a GOR of 500 cf/b shows that a production of 2350 b/d can be obtained on Natural Flow. By intersecting the inflow performance line with the Optimum GOR-line a gas lift production of 2900 b/d is indicated at a required GOR of approximately 1150 cf/b (Fig. 2C). The gas lift gas injection pressure at 10,000 ft would be 2700 psi.

The end of the flowing life is reached when the inflow performance line does not intersect the intake pressure line of the appropriate GOR any more.

This will be the case at a cumulative production of approximately 400,000 bbls. Similarly the end of gas lift life is determined at a cumulative of some 500,000 bbls. A summary of the data which can be determined from Fig. 2 is given below.

TABLE III

PRODUCTION DATA AND LIFE OF WELL ON NATURAL FLOW AND GAS LIFT

		Natural flow		Gas lift					
	Cumulative production	Rates	Production	Rates	Production	Optimum GOR	Gas lift		
							Gas	Gas	Inj. Press.
	(bbls)	(b/d)	(days)	(b/d)	(days)	(cf/b)	(cf/b)	(mcf/d)	(psi)
I	0	2350	99	2900	78	1150	650	1885	2700
II	200.000	1750	111	2200	81	1400	775	1705	2200
III	350.000	950	± 90	1500		1600	850	1275	1750
	400.000	Dead		—	95	—	—	—	—
IV	450.000	—	—	600	± 120	2100	1100	660	1350
	500.000	—	—	Dead	—				
			300						

The producing days are approximated by dividing the production over a certain period by half the sum of the production rate at the beginning and the end of that period.

In the above, Optimum GOR's have been used for the gas lift. Considerable savings in gas lift gas consumption at only a slight loss in production rate may, however, be obtained when GOR's are used somethat the intake pressures, for a certain production rate, increase very little at a decrease of some 200 cf/b below the optimum value of the GOR. See Fig. 2A.

D. Historic development of gas-liquid vertical flow studies

As early as 1930, a theoretical analysis of gas-liquid vertical flow was made, but no solution was found to correlate all the various factors involved and which would fit the wide range of field conditions. This was followed by the development of equations based on small-scale laboratory experiments which proved, to be unreliable, cumbersome, and have a limited range of application.

Gilbert[1]) eliminated the necessity of complex mathematical formulae by establishing, empirically, pressure traverses for production rates up to 600 b/d in five different tubing sizes and a wide range of gas-oil ratios. The application of these purely empirical pressure traverses was limited to relatively low production rates and to fields where the conditions were similar to those on which the curves were based.

A semi-empirical approach was made by Poettmann and Carpenter[3]) who used an energy-balance equation in which the irreversible part of the flow mechanism was related to a simplified Reynolds number, omitting the viscosity; measured field data were used as basis. Total flowing densities of the fluids and the solubility of gas in oil were taken into account but no attempt was made to evaluate the various components which make up the total energy loss. Instaed, a form of analysis was used in which the gas, oil and water were treated as a single phase, and all the significant energy losses could be correlated in a form similar to that of the Fanning equation for frictional losses in single-phase flow. The energy-loss factor was linked to the product of density, velocity and inside diameter of the conduit.

This method was successfully applied in Venezuela to construct a set of annular flow gradients in the La Paz and Mara fields[4]). However, attempts to apply the method to high rates of tubing flow were unsuccessful, since the correlating of Poettmann and Carpenter was based on rather limited data from low-rate measurements which could not be extrapolated in a simple manner to high rates of flow. Subsequently a series of experiments was carried out in a prolific well in the La Paz field in Venezuela with electronic surface-recording instruments to establish a reliable extension of the energy-loss correlation of Poettmann and Carpenter for high rates of flow[5]).

This extended correlation has provided accurate pressure traverses in high-pressure and high-production wells for two-phase vertical flow through both circular and annular conduits.

Pressure traverses calculated with the Poettmann and Carpenter approach will show a reversal of cur-

vature. This is inherent in their basic gradient equation which for one specific conduit size, gas-oil ratio and production rate can be simplified to:

$$\text{gradient} = \text{density} + \frac{\text{constant}}{\text{density}}$$

Thus, with the density increasing with depth, the gradient will initially decrease up to a minimum before it increases at increasing depth. At high production rates the reverse curvature has been confirmed by actual field measurements, but not at low rates for which the traverse with reversed curvature deviates widely from actual measurements.

Furthermore, serious discrepancies were found in wells which produced at a low pressure, a low rate and at high gas-oil ratios, and in wells with viscous crudes.

The deviations from actual measurements are due to the fact that the dimensionless total energy-loss factor of Poettmann and Carpenter was taken as a constant over the whole length of the vertical conduit for one specific rate, gas-oil ratio and conduit size. This factor, however, does change as the type of flow changes over the length of the conduit and with it the contribution to the irreversible losses of each of the two main components, i. e. slip losses between the phases and wall friction losses.

The mechanisms causing slip losses and wall friction losses are apparently different from each other and cannot be related to the total energy loss by using a friction equation but must be separately dealt with.

It was felt that the need for an improved, and more widely applicable, method warranted large-scale laboratory investigations to study further the mechanism of gas-liquid vertical flow. These were started in 1957 and resulted in some 20,000 data points from which new correlations were derived, discussed elsewhere by Ros in 1961[6]).

To deal with the influences of slippage and wall friction separately, use has been made of a pressure-balance equation rather than an energy-balance equation, in which the total gradient is made up of a static gradient, a wall friction gradient and an acceleration gradient.

In the static gradient the effects of slip between the gas and liquid phase are incorporated and are kept separate from the effects due to friction. Moreover, three different types of flow (see later) are distinguished in the vertical flow of oil and gas, and, in principle in each type the slippage and friction function appear in a different manner.

Since 1961 the laboratory measurements have been extended. In particular the mist-flow range pertaining to high gas flow rates was investigated in more detail and the correlations pertaining to this range were refined. Furthermore a correlation was developed for wet oil-gas mixtures. Before these refinements are discussed a brief review of the general picture and the mode of correlating is given.

II. General Picture

A typical example of the results obtained is shown in Fig. 3 for the flow of air and oil (viscosity approx 4cS) through an 8-cm vertical pipe. Both the pressure gradient (solid curves) and the liquid hold-up (dotted curves) have been plotted against the gas throughput for various values of the liquid throughput.

The pressure gradient dp/dh is expressed as a fraction G of the static liquid gradient $\varrho_l g$, thus $G = (1/\varrho_l g)\,(dp/dh)$, where ϱ_l is the liquid density and g the gravity acceleration.

The liquid hold-up, ε_l, is the volume of liquid actually present in a certain pipe section, expressed as a fraction of the total volume of that pipe section. It was measured by means of radioactive tracers and is a measure for the weight of the content of the pipe and thus of the static gradient of the flowing gas-liquid mixture.

The throughputs are characterized by (superficial) velocities v_{sg} and v_{sl}, equal to the in situ volumetric flow rates divided by the total cross-sectional area of the pipe.

As is evident from Fig. 3, the pressure gradient and the hold-up depend strongly on the gas throughput.

At low gas throughput, bubble flow prevails, the liquid phase then being continuous and the gas being dispersed in small bubbles. So long as the volume of the bubbles remains negligibly small, the pipe is full of liquid. Consequently, the liquid hold-up is equal to unity and the pressure gradient nearly equals the static gradient of gas-free liquid; thus also G is approximately equal to unity. Wall friction makes the gradient slightly greater at high liquid flow rates.

At greater gas throughputs, wall friction causes the picture for a low liquid flow rate to differ from that for a high one.

For low liquid rates ($v_{sl} < 40$ cm/sec), increased gas flow initially causes the number and size of the

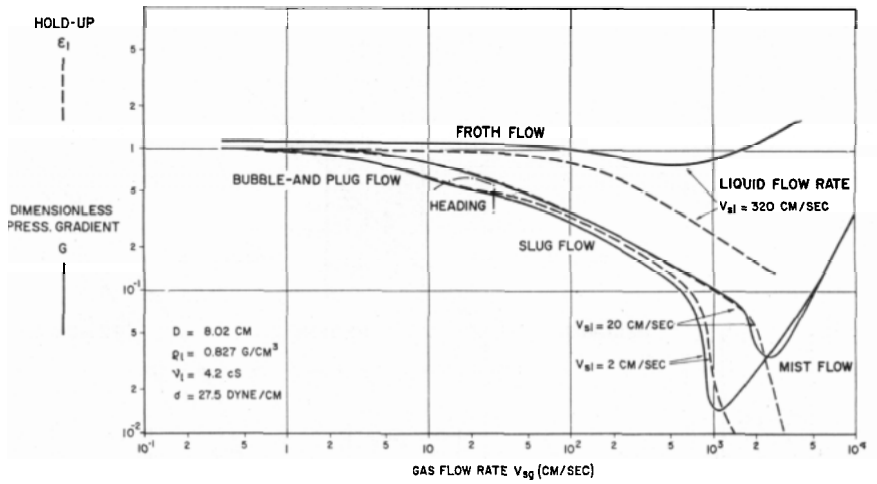

Figure 3 Pressure gradient and liquid hold-up against gas flow and liquid flow.

bubbles to increase until they unite and form bullet-shaped gas plugs, which become unstable and collapse at still higher gas throughputs. Then slugs, containing mainly gas, alternate with slugs containing mainly liquid. All through these flow regions, wall friction remains negligibly small and the pressure gradient, G, consequently nearly equals the liquid hold-up which diminishes, since with increasing gas flow, there is more gas and less liquid in the pipe.

At still higher gas flows ($v_{sg} > 1{,}500$ cm/sec and v_{sl} still smaller than 40 cm/sec), the flow pattern changes from slug flow to mist flow. The gas then becomes the continuous phase with the liquid being transported mainly as droplets in the gas, and for a very small part as a film along the pipe wall. Wall friction makes its appearance, increases sharply with increasing gas flow rate, and far exceeds the ever-diminishing hold-up. Thus the pressure gradient passes a minimum and rises sharply after that.

On increasing the liquid throughput, the picture gradually changes over to the situation of high liquid velocity ($v_{sl} > 160$ cm/sec), where the various flow patterns cannot clearly be discerned. When the gas flow increases from zero, no plug flow can be observed, but the flow becomes turbulent and frothy, with the gas dispersed in an ever increasing number of small bubbles. Only at high gas throughputs does any segregation take place, causing a rapidly repeating slug flow, gradually changing to mist flow at extremely high gas throughputs ($v_{sg} > 5{,}000$ cm/sec). Hold-up decreases only slowly, since with the high liquid throughput the volume of gas in the pipe remains relatively small. The substantial friction, however, increases continuously so that the pressure gradient decreases slowly with increasing gas flow and, after reaching a flat minimum, rises sharply.

In a limited range, the flow in the test installation varied in a cyclic manner. In the case shown in Fig. 3, this occurred for $v_{sl} < 10$ cm/sec and $10 < v_{sg} < 30$ cm/sec. The intensity of this instability, the so-called "heading", was greater the smaller the pipe, the lower the liquid viscosity, and the lower the liquid velocity. Then the heading range was fairly wide and pressure fluctuations were large.

The various flow patterns and heading phenomena only occur in limited zones. These zones can be presented in a diagram in which the transition between the various flow regimes are plotted as a function of gas throughput and liquid throughput. This diagram is shown in Fig. 4. The throughputs are characterized by the velocity numbers of gas and liquid, i. e. RN and N respectively. The lines represent the limits of the correlations given later and practically agree with the transitions between adjoining flow patterns.

III. Correlations

The various flow regimes can be divided into three main regions – those with low, intermediate and high gas throughputs respectively.

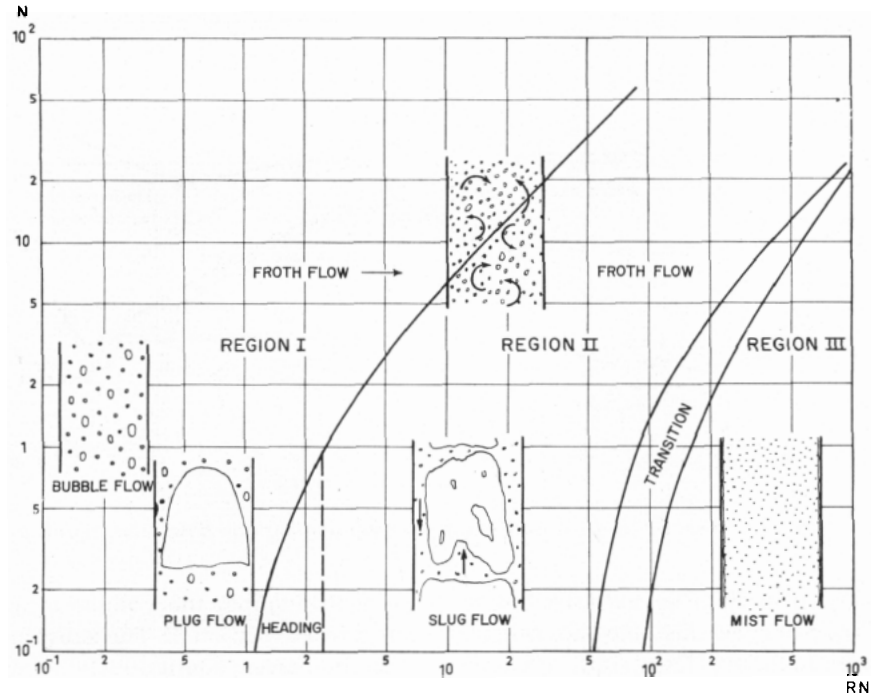

Figure 4 Regions of validity of correlations.

Region I, where the liquid phase is the continuous one, covers bubble flow, plug flow and part of the froth-flow regime.

Region II, where the phases of liquid and gas alternate, covers the slug flow and the remainder of the froth-flow regime.

Region III, where the gas phase is the continuous one, covers the mist-flow regime.

As can be expected, the entirely different nature of these main regions causes the behaviour of both liquid hold-up and friction to be different; in principle, therefore, $3 \times 2 = 6$ different correlations are to be expected.

Both liquid hold-up and friction appeared to depend on the velocities of gas and liquid, (v_{sg} and v_{sl}), the pipe diameter (D) and the liquid viscosity (μ_l). In order to account also for effects of surface tension (σ) and liquid density (ϱ_l), the above governing quantities have been converted into four dimensionless groups:

$$RN = \text{gas velocity number} = v_{sg}\sqrt[4]{(\rho_l/g\sigma)}$$

$$N = \text{liquid velocity number} = v_{sl}\sqrt[4]{(\rho_l/g\sigma)}$$

$$N_d = \text{diameter number} = D\sqrt{(\rho_l g/\sigma)}$$

$$N_l = \text{liquid viscosity number} = \mu_l\sqrt[4]{(g/\rho_l\sigma^3)}$$

IV. Liquid Hold-up

The static pressure gradient, $(dp/dh)_{st}$, in a pipe which is partly (fraction ε_l) filled with liquid and for the remainder with gas, amounts to

$$(dp/dh)_{st} = \varepsilon_l \varrho_l g + (1-\varepsilon_l)\varrho_g g$$

Thus, expressed as a fraction of the static liquid gradient

$$G_{st} = \frac{1}{\varrho_l g}(dp/dh)_{st} = \varepsilon_l + (1-\varepsilon_l)\varrho_g/\varrho_l \qquad (1)$$

The liquid hold-up ε_l is functionally related to the slip velocity, v_s, which is the difference between real average gas and real average liquid velocity and is defined as follows

$$v_s = \frac{v_{sg}}{1-\varepsilon_l} - \frac{v_{sl}}{\varepsilon_l} \qquad (2)$$

For convenience, the slip velocity and not the liquid hold-up has been correlated with the governing groups. Furthermore, the slip velocity, like the other velocities, was expressed in dimensionless form by

$$S = v_s\sqrt[4]{(\rho_l/g\sigma)} \qquad (3)$$

Once S is known, from these relations ε_l and thus $(dp/dh)_{st}$ can be determined.

A. Slip correlation I

The formula which covers the bubble-flow, plug-flow and part of the froth-flow regimes (Region I) reads as follows: —

$$S = F_1 + F_2N + F'_3\left(\frac{RN}{1+N}\right)^2 \qquad (4)$$

In this equation, the dimensionless slip velocity S is correlated to the velocity numbers of liquid and gas, N and RN respectively. The F-factors are constants in specific field applications when viscosity and diameter are given. F_1 and F_2, given in Fig. 5, depend on

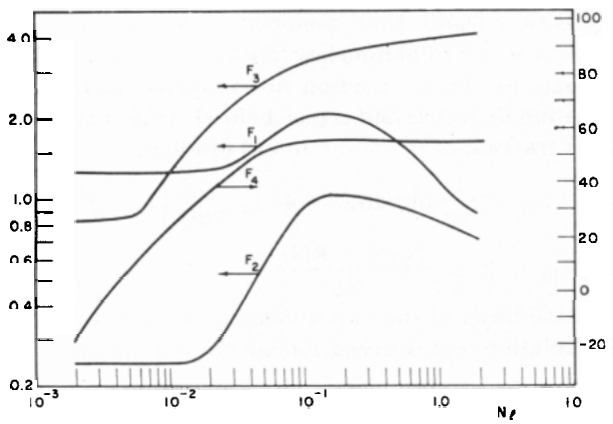

Figure 5
Non-dimensional functions F_1, F_2, F_3 and F_4 against viscosity number N_l

the liquid's viscosity number only. F'_3 depends on both viscosity and diameter and is represented by

$$F'_3 = F_3 - \frac{F_4}{N_d} \qquad (4a)$$

where for flow in pipes the diameter number N_d is based on the internal diameter of the pipe, thus $N_d = D\sqrt{(\rho_l g/\sigma)}$

For flow in annuli, however, N_d should be based on the wetted perimeter, thus on the sum of the internal casing diameter D and the external tubing diameter D_t; therefore in this case $N_d = (D + D_t)\sqrt{(\rho_l g/\sigma)}$.

Region I extends from zero N and RN up to the limit given by

$$RN = L_1 + L_2N \qquad (5)$$

The factors L_1 and L_2 depend on the diameter number and are given in Fig. 6. Again, for flow in annuli N_d should be based on $(D + D_t)$.

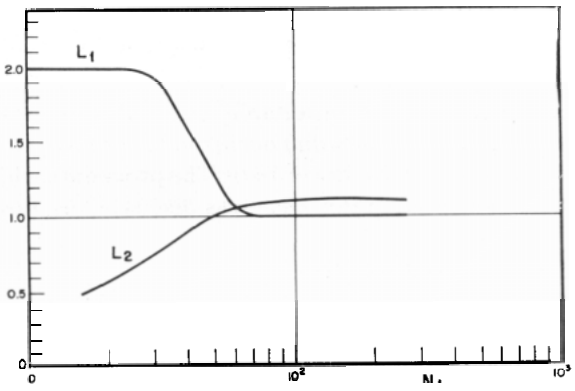

B. Slip correlation II

In the range of intermediate gas throughputs, covering the slug-flow and the remainder of the froth-flow regimes (Region II), the slip correlation reads

$$S = (1 + F_5)\frac{(RN)^{0.982} + F'_6}{(1 + F_7N)^2} \qquad (6)$$

As in the previous correlation, the F-factors become constants when viscosity and diameter are given. F_5 and F_7 are given in Fig. 7, together with F_6 appearing in the expression for F_6', reading

$$F_6' = 0.029\ N_d + F_6 \qquad (6a)$$

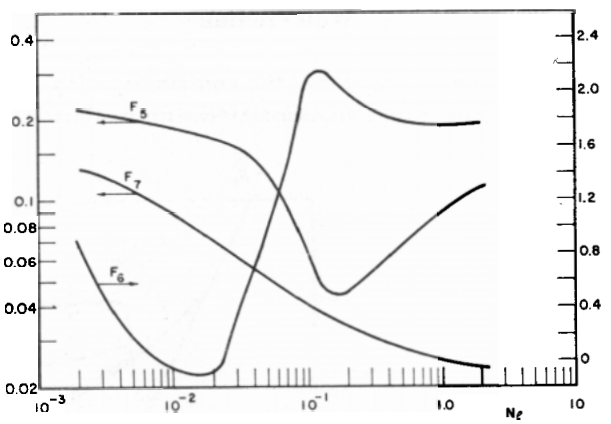

Figure 7
Non-dimensional functions F_5, F_6, and F_7 against viscosity number N_l

Once more, for flow in annuli N_d should be based on $(D + D_t)$.

Region II extends from the upper limit of Region I to the transition zone to mist flow given by

$$RN = 50 + 36N \tag{7}$$

The correlation is unreliable only at low liquid throughput where heading occurred in the laboratory installation near the lower limit. The procedure which may be followed in this case was discussed by Ros[6]).

C. Slip correlation III

For high gas throughputs the gas phase becomes continuous with the liquid being transported mainly as small droplets. This results in virtually no slip between gas and droplets. Therefore,

$$S = 0 \tag{8}$$

From this it follows that $\varepsilon_l = \frac{1}{1+R}$ in which the situ gas-liquid velocity ratio $R = v_{sg}/v_{sl}$. This expression for ε_l in the mist-flow region differs from that given previously in Ref. 6 as the result of the more extensive investigations made since.

Equation (8) is valid in the mist-flow range, characterized by

$$RN > 75 + 84\,N^{0.75} \tag{9}$$

This leaves a gap for the transition zone between slug-flow and mist-flow. For this zone the pressure gradient may be obtained by an interpolation procedure discussed in section VII.

V. Wall Friction

It has been assumed that the contribution $(dp/dh)_{st}$ to the pressure gradient associated with wall friction, results in the Regions I and II from shear stress in the more or less continuous liquid phase and therefore is governed by a Fanning-type of friction law.

A. Friction correlation I–II

The equation governing friction in the Regions I and II was postulated to read

$$(dp/dh)_{fr} = 4 \cdot f_w \frac{\varrho_l v_{sl}^2}{2D}\left(1+\frac{v_{sg}}{v_{sl}}\right)$$

Without slip the real velocity $\bar{v}$ is $(1 + v_{sg}/v_{sl})$ times the superficial velocity v_{sl}, whilst the average density $\bar{\varrho}$ is smaller than the liquid density ϱ_l by the same factor, when omitting the influence of the gas density. Then the assumed relation becomes identical to the Fanning law $(dp/dh)_{fr} = 4 \cdot f_w \cdot {}^1/_2 \bar{\varrho} \bar{v}^2/D$. Effects of slip on friction are reflected in the correlation factors f_2 and f_3 (see below). Thus, expressed as a fraction of the static liquid gradient

$$G_{fr} = \frac{1}{\varrho_l g}(dp/dh)_{fr} = 4 \cdot f_w \frac{v_{sl}^2}{2gD}\left(1+\frac{v_{sg}}{v_{sl}}\right)$$

$$\text{or } G_{fr} = 2 \cdot f_w \frac{N\,(N + RN)}{N_d} \tag{10}$$

On the basis of the experimental data the following correlation was derived for the friction factor f_w

$$f_w = f_1 \frac{f_2}{f_3} \tag{11}$$

The friction factor is mainly governed by f_1 which is given in Fig. 8 as a function of the Reynolds number of the liquid $Re_l = \varrho_l v_{sl} D/\mu_l$. As in equation (10), D is the hydraulic diameter D_h of the flow string. Thus, for annuli $D_h = D - D_t$ and $N_d = (D-D_t)\sqrt{(\varrho_l g/\sigma)}$.

Figure 8 is identical to the well known Moody[7]) diagram for single-phase flow, except in the

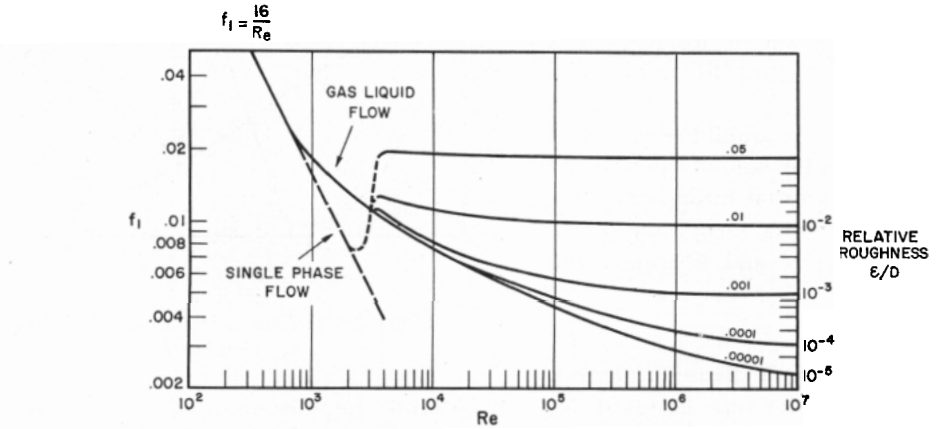

Figure 8 Non-dimensional function f_1 against Reynolds number Re

transition range between laminar and turbulent flow. The effect of relative wall roughness ε/D, though for ε ≈ 10^{-3}D (as in tubing) a factor of secondary importance, is shown as well.

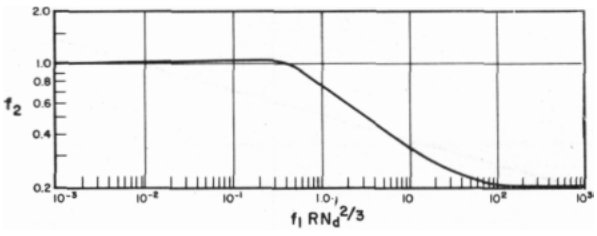

Figure 9
Non-dimensional function f_2 against $f_1RN_d^{2/3}$

Factor f_2 is a correction for the in situ gas-liquid ratio R and is given as a function of the group $f_1RN_d^{2/3}$ in Fig. 9. The value of f_2 is nearly equal to unity when R is small, but decreases sharply when R becomes high.

Factor f_3 is a further correction of the second order for both liquid viscosity and in situ gas-liquid ratio and equals $1 + f_1\sqrt{(R/50)}$. In the usual R-range the influence is of importance only for viscosities higher than some 50 centistokes.

The friction correlation I—II is valid in the regions I and II and covers the heading range as well; thus, from zero N and RN up to the limit given by RN = 50 + 36 N.

B. Friction correlation III

In the mist-flow range, where $RN > 75 + 84\,N^{0.75}$, the gas phase is continuous and friction originates from the drag of the gas on the pipe wall. Thus, the friction gradient should be based on the gas phase

$$(dp/dh)_{fr} = 4 \cdot f_w \frac{\varrho_g v_{sg}^2}{2D}$$

and $$G_{fr} = \frac{1}{\varrho_l g}(dp/dh)_{fr} = 4 \cdot f_w \frac{\varrho_g}{\varrho_l}\frac{v_{sg}^2}{2gD}$$

or $$G_{fr} = 2 \cdot f_w N_\rho \frac{(RN)^2}{N_d} \qquad (12)$$

where $N_\rho = \varrho_g/\varrho_l$ is a density influence number.

In analogy to the formula for the Regions I and II, here a factor $(1 + v_{sl}/v_{sg})$ should be added. It was omitted since with mist-flow $v_{sg} >> v_{sl}$ and the effect of liquid throughput disappears, see Fig. 3.

Since slip is absent, the friction factor should be that given in the Moody diagram of Fig. 8, now, however, as a function of the Reynolds number of the gas stream $Re_g = \varrho_g v_{sg} D/\mu_g$. Thus, the correlation reads

$$f_w = f_1 . \qquad (13)$$

With mist-flow the "wall" roughness, ε, is the roughness of the liquid film which covers the wall of the pipe. This film is highly corrugated, offers a high resistance to the gas flow and is the cause of the greater part of the pressure gradient. The problem, therefore, has shifted to determining ε. Previously (see Ref. 6) this roughness was taken to be constant. Further investigation, however, showed that relations were more complicated.

The ripples of the wall film result from the drag of the gas deforming the film in opposition to the surface tension. Such a process will be governed by a dimensionless group:

$$We = \frac{\rho_g v_{sg}^2 \varepsilon}{\sigma} \qquad (14)$$

This Weber number will be a function of the operating variables. Once its value has been established, ε may be derived from equation (14). As a first approximation the Weber number may be taken constant, We = 34. Liquid viscosity, however, was found to affect its magnitude. This could be accounted for by making We a function of the dimensionless group $N_\mu = \mu_l^2/\varrho_l\sigma\varepsilon$ which reflects the interaction between viscosity and surface tension. In Fig. 10 We is given as a function of the product of We and N_μ, which product is independent of ε.

In the mist-flow range and for high values of v_{sg} the roughness ε becomes extremely small. However, the effective roughness never becomes smaller than that of the pipe itself, some 10^{-3}D. At the other end, at the transition to slug-flow, the waviness of the film may become extremely great with the crests of opposite waves touching and forming liquid bridges. Then ε/D approaches 0.5. The corresponding values for f_1 may be found by extrapolation of the Moody diagram for $\varepsilon > 0.05\,D$ by means of the formula

$$f_1 = \frac{1}{\{4 \cdot \log_{10}(0.27\,\varepsilon/D)\}^2} + 0.067\,(\varepsilon/D)^{1.73} \qquad (15)$$

With such great waves on the wall the passage for the gas will be perceptibly restricted. As a refinement, therefore, D−ε could be substituted for D throughout the calculation of the friction gradient, and $v_{sg}D^2/(D-\varepsilon)^2$ for v_{sg}. In that case ε follows from an iteration process.

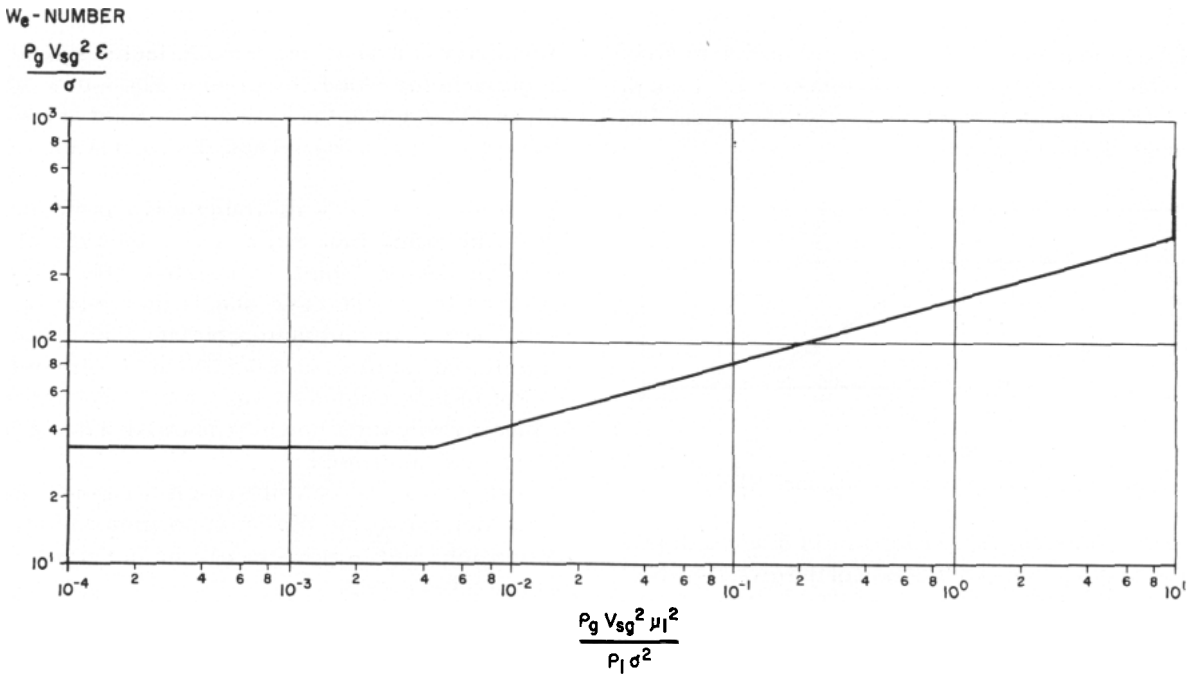

Figure 10 Correlation for the film-thickness ε under mist-flow conditions

VI. Acceleration

Acceleration fortunately is so small that in nearly all circumstances it may be neglected for flow in wells (see Refs. 3 and 4). It is only in the mist-flow range that it cannot always be discarded. This may be evaluated as follows.

The acceleration gradient reflects the change in momentum when the mixture is accelerated vertically. In the mist-flow range slip is absent and the velocities are equal to v_{sg}, since in case acceleration is of importance, velocities are so high that the effect of wall film thickness on velocities may be neglected. The mass flow rate is of course constant and equal to $\varrho_l v_{sl} + \varrho_g v_{sg}$, so that the acceleration gradient is

$$(dp/dh)_{ac} = -(\varrho_l v_{sl} + \varrho_g v_{sg})\ (d\, v_{sg}/dh)$$

In presence of suspended liquid, gas expansion will be isothermal, and thus the product pv_{sg} will be constant. Therefore

$$v_{sg}\ (dp/dh) + p\ (d\, v_{sg}/dh) = 0.$$

From these, with $(1/\varrho_l g)\ (dp/dh) = G$, follows for the reduced gradient

$$G_{ac} = \frac{1}{\varrho_l g}(dp/dh)_{ac} = (\varrho_l v_{sl} + \varrho_g v_{sg})\frac{v_{sg}}{p}G \quad (16)$$

Since the total gradient, expressed as a fraction of the static liquid gradient $G = G_{st} + G_{fr} + G_{ac}$ it follows that

$$G = \frac{G_{st} + G_{fr}}{1 - (\varrho_l v_{sl} + \varrho_g v_{sg})\ (v_{sg}/p)} \quad (17)$$

The acceleration thus may be accounted for by correction of the pressure gradient resulting from hold-up and friction by a factor which may become of importance at low pressure and high gas velocity, thus for the upper part of the flow string.

VII. Pressure Gradient

Determination of the total pressure gradient in the Regions I, II or III will offer no difficulty, since it is equal to the sum of the static gradient and the friction gradient, if necessary corrected for acceleration as indicated by formula (17).

For RN values in the transition zone between slug-flow and mist-flow the pressure gradient can be approximated by linear interpolation, on the basis of the value of RN, between G-values obtained for $RN = 50 + 36\,N$ and $RN = 75 + 84\,N^{0.75}$, at the boundaries of Region II and III respectively.

In doing so, best results are obtained if it is taken into account that the gas mass flow rate $\varrho_g v_{sg}$ should be a fixed quantity. Thus, if v_{sg}' is the gas velocity which corresponds with the RN value at the boundary, $\varrho_g' v_{sg}' = \varrho_g v_{sg}$, or $\varrho_g' = \varrho_g v_{sg}/v_{sg}'$. This correction of

the gas density for use at the boundary in the interpolation procedure is of importance at the mist-flow limit, since with mist-flow gas density affects the friction. With slug-flow gas density has very little effect, so that the correction need not be applied at the limit to slug-flow.

VIII. Wet Mixtures

The correlations presented are intended for use with dry oil/gas mixtures. Owing to the use of dimensionless groups, effects of surface tension and liquid density have been accounted for. The same correlations, therefore, should apply also to the flow of water and gas. This has appeared to be correct, though with reduced but still useful accuracy.

With wet mixtures the pressure gradient will be unpredictable when the oil and water form stable emulsions. If, however, the water phase separates readily from the oil phase it would seem feasible to predict by means of interpolation the gradient $(dp/dh)_{ow}$ of an oil/water/gas mixture from the gradient $(dp/dh)_o$ of a dry oil/gas mixture and the gradient $(dp/dh)_w$ of a water/gas mixture, all three for the same total liquid throughput. This indeed was found to be the case and for a water content c_w (on total liquid), the pressure gradient for the wet mixture may be found from

$$(dp/dh)_{ow} = (1-7.3\,c_w)\,(dp/dh)_o + 7.3\,c_w\,(dp/dh)_w \quad (18)$$

The relation is valid for the Regions I and II and water contents of less than 10 %. With the high velocities prevailing in Region III emulsions will be formed, particularly in the liquid film on the wall. These emulsions greatly affect the roughness of the film and thereby the pressure gradient. The reason for the failure of Equation (18) to predict the gradient correctly at high water contents is quite different. Even though water and oil may readily separate, a small quantity of oil ($<<1$ %) will remain finely dispersed in the water and give it a milky appearance. This milky water behaved differently from pure water. Notably the heading range, which with pure water is rather wide, was appreciably smaller with the milky water. Furthermore, in and also below the heading range (smaller v_{sg}) in the upper part of Region I rather large discrepancies, up to 30 %, in the gradients for pure water and milky water have occasionally been found. All this makes the gradient for pure water unsuitable for correlation purposes when the water content of a wet mixture rises over 10 %.

IX. Discussion

The correlations given for Region I fitted the laboratory measurements for dry mixtures with a standard deviation of 3 %, which is equal to the measuring accuracy. In Region II the unstable and pulsating character of the flow increased the deviations to 8 %. The refinements in the correlations for mist-flow reduced the standard deviation from the 10 % of the previous correlation[6]) to 6 %. With wet mixtures containing less than 10 % of water, the discrepancy in the Regions I and II amounted to 10 %.

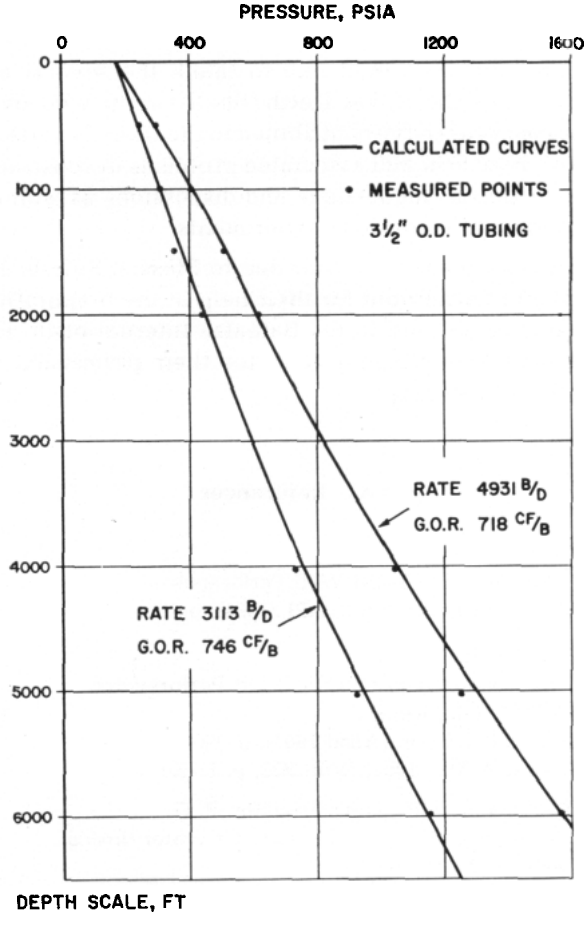

Figure 11
Comparison between measured points and calculated curves

The results obtained look promising, but — as discussed in reference 6 — there are a number of factors which may cause the pressure gradients in a well to differ from those in a laboratory installation. The salient points are at present being checked in field tests. What data are already available are encouraging. An example is given in Fig. 11, where for a high potential well in the La Paz field in Venezuela the calculated pressure traverses, using the above correlations, have been compared with the measured ones for two different flow rates.

The computation of these pressure traverses is extremely laborious. For that reason a computer program has been made and therefore the intricacy of the formulae to be evaluated is of little importance.

X. Acknowledgement

The authors would like to thank the several engineers of the Royal Dutch / Shell Group who over the past years have contributed to the study of vertical two-phase flow and associated problems in constructive criticism, suggestions and discussions as well as in field and laboratory experiments.

Special thanks are also due to Messrs. Stillebroer and van Oosterhout for their help in the preparation of this paper, and to the Bataafse Internationale Petroleum Maatschappij N.V. for their permission to publish this study.

XI. References

1. Gilbert, W. E.
"Flowing and Gaslift Well Performance",
Drill. and Prod. Pract., API (1954), p. 126.

2. McAfee, R. V.
"The Evaluation of Vertical Lift Performance in Producing wells",
Journ. Pet. Tech. (April 1961), p. 390.
Trans. AIME (1961), Vol. 222, p. I—391.

3. Poettmann, F. H., and Carpenter, P. G.
"Multiphase Flow of Gas, Oil and Water through Vertical Flow Strings",
Drill. and Prod. Pract., API (1952), p. 257.

4. Baxendell, P. B.
"Producing Wells on Casing Flow",
Trans. AIME (1958), Vol. 213, p. 202.

5. Baxendell, P. B., and Thomas, R.
"Calculation of Pressure Gradients in High-Rate Flowing Wells",
Journ. Pet. Tech. (Oct. 1961), p. 1023.

6. Ros, N. C. J.
"Simultaneous Flow of Gas and Liquid as encountered in Well Tubing",
Journ Pet. Tech. (Oct. 1961), p. 1037.

7. Moody, L. F.
"Friction Factors in Pipe Flow",
Trans. ASME (1944), Vol. 66, p. 671.

This paper was presented on June 25, 1963 by H. DUNS JR.

Discussion

H. J. GRUY *(H. J. Gruy and Associates, Inc., Dallas, Texas, USA).* The authors have made an excellent contribution to the literature and should be congratulated on their work. We would like to point out to those working on this problem the work done by Ovid Baker and Will Swerdloff and published in the *Oil and Gas Journal,* May 16, 1955, pp. 148–163. They worked with two-phase flow in horizontal pipes in connection with bringing oil and gas to shore from producing wells located in the Gulf of Mexico.

We were unfamiliar with their work in 1957 when we had to predict capacities of some West Texas flowing wells in connection with a multimillion dollar lawsuit. We made field measurements of the flowing bottom hole and wellhead pressures and production rates of oil and gas and calculated the expected pressure drops using the techniques available at the time on vertical two-phase flow. These calculations showed much greater pressure drops than those actually measured. The published correlations which we would find showed that the wells should not have been capable of flowing at that time. Naturally a prediction of future conditions could not be made with methods that did not match known conditions. A further search of the literature revealed the published work of Ovid Baker and Will Swerdloff referred to previously.

The Baker and Swerdloff correlations with added gravity factors to convert from horizontal to vertical conditions resulted in an excellent check of the measured field data. We had Productivity Index data consisting of flowing bottom hole pressures and production rates of oil and gas on 72 wells, all producing

from Canyon Reef lime of Pennsylvanian age at a depth of approximately 6,700 feet. Static bottom hole pressures varied from 2400 to 3200 pounds per square inch, oil rates varied from 80 to 1500 barrels per day, flowing tubing pressures varied from 325 to 1265 pounds square inch and gas-oil ratios varied from 800 to 2100 cubic feet per barrel.

These comments are offered primarily because the Baker and Swerdloff work is not referenced in this paper. We believe that it is useful and should be called to the attention of those concerned with this problem.

H. DUNS *replies.* Since the referenced article is on horizontal *gas* flow only it is assumed that Mr. Gruy probably is referring to an article by Mr. Ovid Baker "Designing Pipelines for simultaneous Flow of Oil and Gas", Oil and Gas Journal, 26/7/54 and with which Mr. Ros and I are both familiar.

It is really most surprising that by a simple addition of gravity influence only to account for the conversion from horizontal to vertical flow, and for such a wide range of conditions, a good check with the measured field data was obtained. We would certainly be very interested to receive more pertinent data about these wells and the method of calculation followed by you, so that we can compare the results with Mr. Ros' method of calculation.

M. SCHEPERS *(Shell-BP, Nigeria).* In the calculations use has been made of a Pressure Balance Equation instead of an Energy Balance Equation as was done by Poettmann and Carpenter. Has that any specific advantage?

H. DUNS *replies.* Yes, because the Pressure Balance Equation offers the possibility to define the pressure gradient by means of the two main mechanisms causing pressure losses, i. e. the volumetric distribution of the phases and the drag along the pipe wall. Such a definition is useful since both phenomena can be measured.

With an Energy Balance Equation, however, the pressure losses must be derived from a detailed knowledge of the energy exchange between the phases, which is not yet available. Application of simplified methods like those suggested by Poettmann and Carpenter will, as a rule, produce accurate predictions in a limited range only.

A. PAUL SZILAS *(Miskolc — Egyptemváros, Hungary).* I should like to congratulate the authors on their excellent paper and would also like to have their opinion on the following points:

1) Are the deviations between measured and calculated data, using Poettmann and Carpenter's method, not due to the fact that at small production rates slippage and at large production rates friction is the deciding factor, whereas the Fanning type friction equation, as used by Poettmann and Carpenter, can only be applied for calculation of friction losses?

2) Do the authors plan to publish the calculation method in the near future?

3) Do the authors have any experience about the degree of error introduced by the assumption that the two-phase vertical flow in the well is isothermic instead of polytropic, especially at small production rates?

H. DUNS *replies.* 1) Yes, that is correct. The reason for the large deviations in the pressure gradient calculation when using the Poettmann and Carpenter method at small production rates is that in the latter method only one single constant energy-loss factor was taken over the whole length of the vertical conduit for one specific rate, gas-oil ratio and conduit size. This factor depends, however, also on liquid viscosity and furthermore changes as the type of flow changes over the length of the conduit. At high production rates, where indeed the wall friction is the predominant contributor to the pressure gradient, the energy loss factor is nearly constant throughout the flow string.

2) It is not intended to publish the computer program for the method of calculation developed by Mr. Ros.

3) Whether the flow in a well is isothermal, polytropic or otherwise depends largely on liquid production rate, geothermal gradient and heat transfer to and heat penetration in the rock surrounding the well bore. Such processes can be studied analytically, but the calculations are rather intricate. In our approach we made use of the empirically observed fact, that the temperature profile in the flow string can be approached with reasonable accuracy by a linear relationship with depth.

In the method described in the paper a vertical temperature gradient is therefore derived (and used) from measured bottom hole and well head temperatures. If these are not available a best estimate is made.

No data are available on the degree of error but this could of course be derived from the suggested method of calculation.